Identification of the State of a Fluidized Bed by Pressure Fluctuations

O. Trnka, V. Veselý, and M. Hartman
Institute of Chemical Process Fundamentals, Academy of Sciences of the Czech Republic, 165 02 Prague 6-Suchdol, Czech Republic

Z. Beran
LEAR Corp., 636 00 Brno, Czech Republic

A novel approach was used for the on-line characterization of the state of a fluidized bed. The treatment technique using the Fast Fourier Transform of measured pressure fluctuations was developed to create plots describing the evolution of bed behavior from fixed bed to pneumatic transport. A new triad of quantities proposed are: divide ratio (degree of dominancy) of amplitude spectrum, square root of spectrum power of pressure fluctuations, and gas velocity. The technique was demonstrated on gas fluidization of solids having a wide size distribution composed of irregularly shaped solids.

Introduction

Fluidization has long been recognized as an efficient means of contacting gas and particulate solids. The performance of fluidized-bed units is affected strongly by the flow regime in the vessel. The analysis and description of flow or contacting pattern in gas–solid contacting units, where a gas flows upward through a bed of solids, can be found in the literature (such as Catipovic et al., 1978; Grace, 1986, 1990; Hartman and Veselý, 1993; Hartman et al., 1995).

The flow regime or contacting mode varies widely, depending on the particle size, particle density and particle geometry, gas density and gas viscosity, and gas velocity and column architecture. In general, the fluidized beds can be operated in six different regimes: particulate/homogeneous fluidization (Group A powders of the Geldart classification only), bubbling fluidization, slugging fluidization (smaller vessels only), turbulent fluidization, fast fluidization, and pneumatic conveying. The bubbling beds can be further classified into three different modes of contacting: fast bubble regime, slow bubble regime, and rapidly growing bubble regime. Our experience indicates that transitions between the respective modes are not often sharp. In practical situations, effects of the particle-size distribution and/or particle-density distribution also have to be considered.

To distinguish between the different flow regimes of gas–solid fluidization, several experimental properties can be observed or measured, such as visual appearance, bed expansion, local voidage fluctuations, or pressure fluctuations (such as Brereton and Grace, 1992). A few years ago, Yates and Simons (1994) presented an extensive review of experimental methods, probes, and sensors available for the investigation of the flow of gases and solids in the fluidized suspensions.

The literature indicates that quite detailed information on system hydrodynamics can be deduced from the study of pressure fluctuations within the bed (such as Svoboda et al., 1983, 1984; Chehbouni et al., 1994; Bai et al., 1996a,b; Svensson et al., 1996; Briens et al., 1997; He et al., 1997; Schouten and van den Bleek, 1998; Xu et al., 1998). It is generally accepted that these fluctuations are due mainly to dynamics of the random motion of heterogeneities such as gas pockets (bubbles) and particle clusters in fluidized gas–solid suspensions (He et al., 1997; Xu et al., 1998). However, the exact details of cause and effects are still the source of considerable discussion.

We expect that the effect of variables such as gas velocity, gas–solids material properties, bed height, and bed architecture on the mode of fluidization can be inferred from their influence on the pressure fluctuations. Although spectral analysis of the fluctuations of pressure can be employed to characterize different states of fluidization (such as Svensson et al., 1996), to the best of the authors' knowledge, it has not yet been reported in the literature as being used for on-line monitoring. This is one of the reasons Schouten and van den Bleek (1998) mention that quantification of the time series' dynamics through some invariant is not always straightforward.

Correspondence concerning this article should be addressed to M. Hartman.

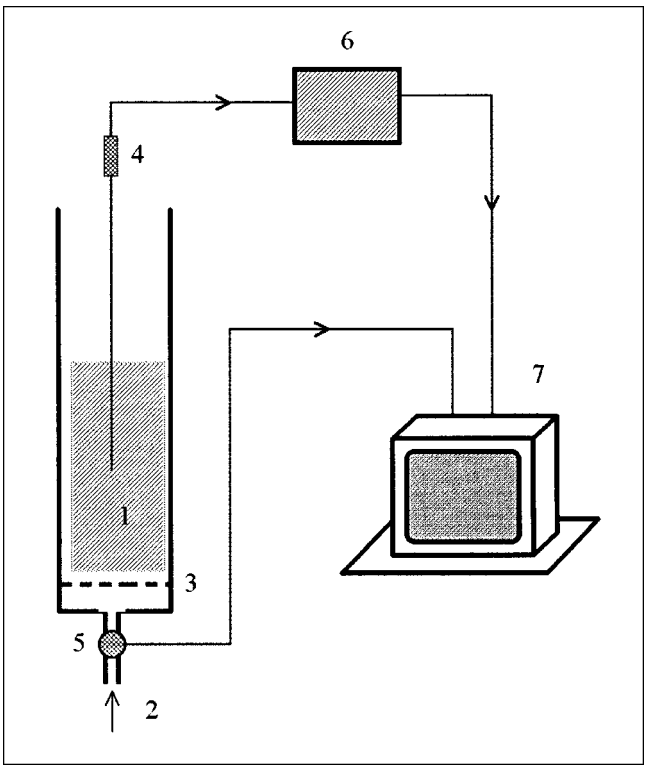

Figure 1. Experimental system.

1, Fluidized bed; 2, inlet of air; 3, perforated plate distributor; 4, pressure probe; 5, flowmeter; 6, analog/digital convertor; 7, computer.

In this work, the pressure fluctuations are measured within the fluidized bed and the amplitude spectra are used for monitoring different states of fluidization, varying from bubbling fluidization to the verge of pneumatic transport. The objective of this study was to find and explore a feasible way of determining the mode of fluidization based upon on-line evaluation of amplitude spectra of the pressure fluctuations.

Experimental Studies

Apparatus

The principal component of the experimental apparatus shown in Figure 1 was a cylindrical glass column of 8 cm ID and height 400 cm. The column was equipped with an interchangeable, sandwiching perforated-plate distributor of free area 2–12% and orifice diameter 0.8 mm. Every care was taken to ensure a uniform gas distribution. Air passed through an oil filter, drier, and orifice meter or rotameter before it entered the bottom of the column. The superficial velocity of air could be increased up to 4 $m \cdot s^{-1}$.

Pressure probes were inserted through taps installed along the height of the column. Four-mm-ID stainless-steel tubes, the ends of which were covered with a wire gauze, proved to be adequate, and no significant damping or resonance effects in these probes were detected. In preliminary experiments, the influence of the location of the pressure probe in the bed was tested. While the effect of radial position was found to be insignificant, the pressure amplitudes were significantly influenced by the axial position of the probe. In all experiments, the pressure probe was located at 8.5 cm above the gas distributor.

The outside opening of the probe was connected to a piezoelectric pressure transducer that produced an output voltage proportional to the pressure signal. The output signal, measured relative to the average pressure, was amplified, converted to a digital form, and further processed on-line by a personal computer. The digital signal was treated by the computer in the time windows as long as 4 s with a sampling frequency of 128 Hz. A discrete spectrum of the fluctuations was computed for each time window. The spectrum includes discrete spectral lines from the interval [0.25 Hz, 32 Hz], with a step of 0.25 Hz per line. The response frequency of the employed pressure transducer was of the order of 1 kHz. The probe measured the pressure with a maximum overall error of 1%.

In the course of all experimental runs, the velocity of air was at first gradually increased from $U = 0$ to U_{max} (maximum of 3.5 $m \cdot s^{-1}$), above which the elutriation of solids out of the column starts. Then the experiment continued by decreasing U back to $U = 0$. No hysteresis phenomena have been observed. The experiments were always performed at three different heights of fixed (poured) bed: 10, 12 and 15 cm. Air was used as a fluidizing gas at ambient temperature 20–22°C.

Particles

Different materials such as ballotini (glass beads), ceramsite, and bentonite were chosen for the experimental measurements. In order to cover all three basic regions of the Geldart diagram, fractions of different size were employed, as summarized in Table 1.

The measured data were interpreted through characteristic curves developed in this work. As all such curves were very similar for the respective solids, only results obtained with ceramsite are presented. Such particles are quite close to the materials often employed in large fluidized beds. Physical properties of ceramsite particles are presented in Tables 2 and 3.

Procedure

The voltage–time signals corresponding to the pressure–time signals were collected for a period of time at a given gas flow rate, see Figure 2a. By means of the fast (discrete) Fourier transform (FFT) of the fluctuating pressure signal, we obtained an amplitude spectrum (such as Press et al., 1992) that expresses the distribution of amplitude with frequency as

Table 1. Tested Solids

Geldart Group	Material	Particle Size d_{pj} (mm)
A	Ballotini	0.10–0.12
A/B	Bentonite	0.40–0.60
B	Ballotini	0.60–0.90
B/D	Bentonite	0.80–1.20
B/D	Ceramsite	0.40–2.40
D	Ceramsite	1.80–3.60

Table 2. Size Distribution of Ceramsite Particles Used in Experiments

Sieve Aperture (mm)	Particle Size, d_{pj} (mm)	Wt. % in Range	Cumul. % Undersize
−2.8+2	2.4	14.5	100
−2+1.2	1.6	14.6	85.5
−1.2+1	1.1	15.9	70.9
−1+0.8	0.9	14.3	55.0
−0.8+0.5	0.65	29.4	40.7
−0.5+0.36	0.43	9.8	11.3
−0.36+0.18	0.27	1.5	1.5

shown in Figure 2b. Then the lines in the amplitude spectrum were assorted in the degressive order as illustrated in Figure 2c for the frequencies between $f_{\min} = 0.25$ Hz and $f_{\max} = 32$ Hz. The median of this assorted spectrum, f_M, was computed according to Eq. 1

$$f_M = f_{i_M}, \tag{1}$$

in which i_M complies with

$$\sum_{i=1}^{i_M} a_i = \sum_{i=i_M+1}^{n_{FFT}} a_i. \tag{2}$$

A position of the median, f_M, is also shown in Figure 2c.

Fluctuation model and results

In addition to the gas velocity, U, two quantities, deduced from the assorted amplitude spectrum, were chosen to describe the state of fluidized bed:

1. The quantity E, defined as square root of the spectral power of the pressure fluctuations in the chosen frequency band, or

$$E = \sqrt{W} \tag{3}$$

where

$$W = \frac{t_{\text{sig}}}{n_{FFT}} \cdot \sum a_i^2. \tag{3a}$$

2. The divide ratio of the amplitude spectrum, M, defined as

$$M = 1 - f_M/f_{\max} \tag{4}$$

Table 3. Physical Properties of Ceramsite Particles

Particle density, ρ_p (kg·m^{-3})	1570
Bulk density of loosely packed bed (kg·m^{-3})	985
Minimum fluidization velocity,* U_{mf} (m·s^{-1})	0.38
Velocity at beginning fluidization,* U_{bf} (m·s^{-1})	0.33
Complete fluidization velocity,* U_{cf} (m·s^{-1})	0.51
Superficial velocity at which entrainment begins,* U_{be} (m·s^{-1})	2.15

*Measured with air at ambient conditions: 20°C, 0.1 MPa.

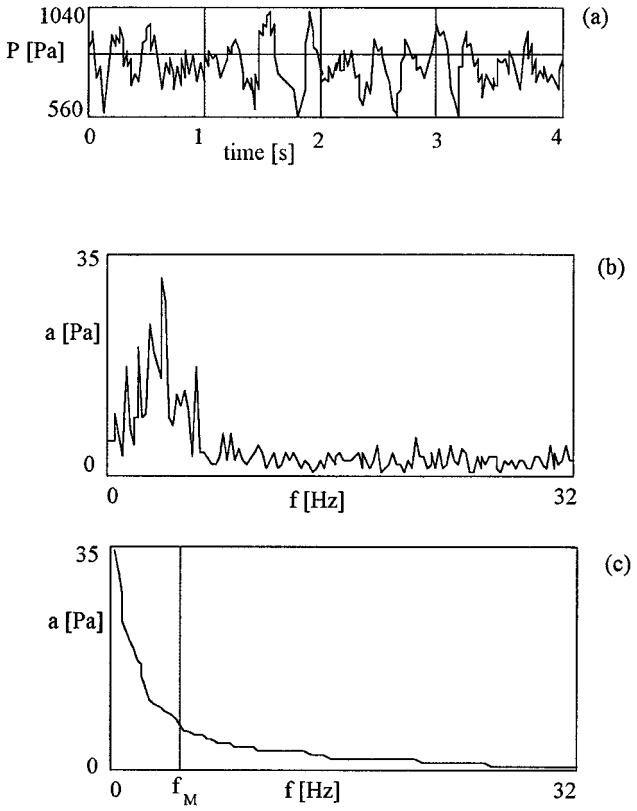

Figure 2. Measured pressure fluctuations and their treatment.

(a) Pressure signal in the used time window. Length of window $t_{\text{sig}} = 4$ s, number of samples in the window $n_{\text{sig}} = 512$; (b) amplitude spectrum of the chosen band of frequency $\langle f_{\min} = 0.25$ Hz, $f_{\max} = 32$ Hz$\rangle$ with corresponding number of lines in the spectrum as large as $n_{FFT} = 128$; (c) amplitude spectrum assorted degressively by the amplitude with the marked median f_M. Bubbling bed, $U = 0.35$ m·s^{-1}, $M = 0.83$.

The quantity, M, occurring in the interval $M \in [0.5, 1]$, has the following features:

- If a fluctuating signal represents the random fluctuating signal in a given time window, then $M \cong 0.\bar{6}$. By this term we mean a fluctuating signal with random, uniformly distributed amplitudes. The assorted amplitude spectrum of such a signal forms a triangle for which it is apparent that M is as large as just mentioned.
- For the signals that make up dominant frequencies, M lies on the interval $M \in [0.\bar{6}, 1]$.
- For the signals with a single dominant frequency, it holds that $M \to 1$.
- The divide ratio, M, can be viewed as a measure of dominancy of the spectrum. Its value suggests whether there are pronounced dominant lines in the spectrum or not.

As shown earlier, the proposed model assumes that an actual state of the pressure fluctuations within the fluidized bed can be described with the aid of three quantities (attractors) $E(U)$, $M(U)$, and U. The first two quantities are given by the behavior of the bed; the superficial gas velocity, U, is an independent, operation parameter, which can easily be controlled. The triad defines a position of an operation point $P = [E, M, U]$ in the tridimensional space $E \times M \times U$. Any

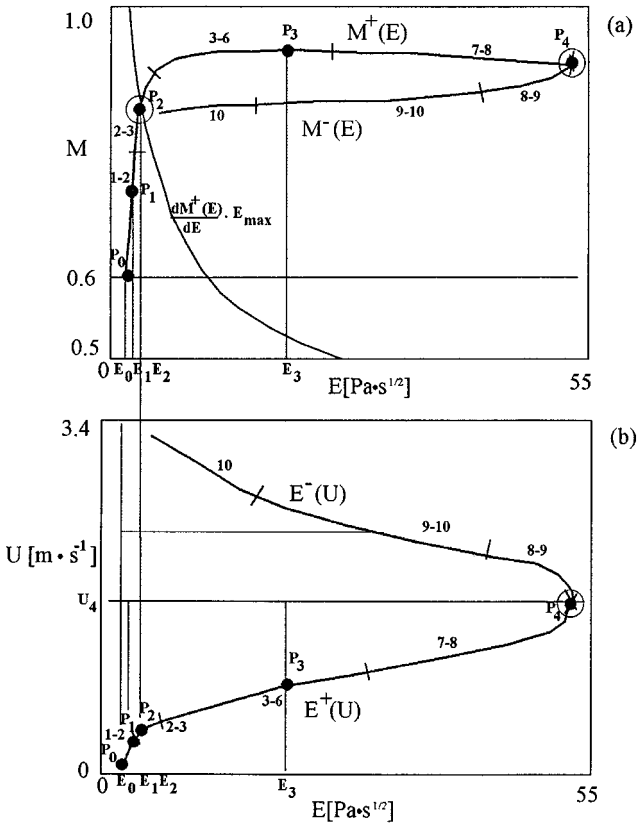

Figure 3. Characteristics of the fluctuation model of fluidized bed in 3-D space $E \times M \times U$ for ceramsite (0.40–2.40 mm).

(a) Projection onto the $E \times M$ plane and graph of the quantity M vs. E [function $(dM^+/dE) \cdot E_{max}$]; (b) projection onto the $E \times U$ plane and dependence of E on the gas velocity U [the maximum at $U = U_4 \equiv U_{be}$ divides the graph into two branches $E^+(U)$ and $E^-(U)$].

change in position of the operation point is closely related to the change in the operation regime of a fluidized bed under investigation.

When the superficial gas velocity, U, is gradually increased from $U = 0$ to $U = U_{max}$, the operation point $P(U) = [E(U), M(U), U]$ moves along a characteristic curve (see Figures 3a and 3b). This trajectory can be called the characteristics of fluidized bed that do not change as long as the physical parameters of bed remain unchanged. Our experimental data, amassed with a variety of materials, indicate that such characteristic curves can be employed in detecting different operation regimes of fluidized beds.

As can be seen in Figure 3a, the characteristics of the bed cannot be expressed by a single function dependence such as $M = M(E)$, nor by the inversion function $E = E(M)$. As shown in Figure 3b, $E(U)$ increases when U is increased from $U = 0$ to a certain value of $U = U_4$. For $U > U_4$, the function $E(U)$ decreases with the increasing U. The functions $M^+(E)$ and $M^-(E)$ in Figure 3a and functions $E^+(U)$ and $E^-(U)$ in Figure 3b are related to $U \le U_4$ and $U \ge U_4$, respectively.

As shown in Figures 3a and 3b, there are five characteristic points $(P_i = [E_i, M_i, U_i], i = 0\text{–}4)$ on the curves $M(E)$ and $U(E)$ of the fluctuation model.

The point $P_0 = [E_0, 0.6, 0]$ corresponds to $U = 0$. In practice, however, the energy of the spectrum is not zero, and the divide ratio $M \cong 0.\bar{6}$ corresponds to the random fluctuating signal of the background. This point represents a position of the ever-present background of different origin. Nevertheless, the point P_0 is useful and can easily be determined.

The point $P_1 = [E_1, M_1, U_1 = U_{bf}]$ represents the beginning fluidization velocity, which is defined and determined by the standard (classic) method (such as Hartman and Coughlin, 1993). Visual observations indicate that first very small bubbles are formed in a mostly static bed of solids, as mentioned in Figure 4 (regime 2^-).

The point $P_2 = [E_2, M_2, U_2 = U_{cf}]$ marks a transition to the regime 2^+ in Figure 4 in which a state of complete (total) fluidization is attained, where practically all the solids are in movement. At this point, the bubbles passing through the bed still remain quite small. Our empirical experience, gained in the course of experiments, made it possible to define the position of point P_2 with the aid of Eq. 5

$$M^+(E) = \frac{dM^+(E)}{dE} \cdot E_{max}, \qquad (5)$$

that is, as the intersection of the function $M^+(E)$, with its derivative multiplied by the maximum value of function $E(U)$, or E_{max}. The position of P_2 can be viewed as a balance between the standstill state and that of motion.

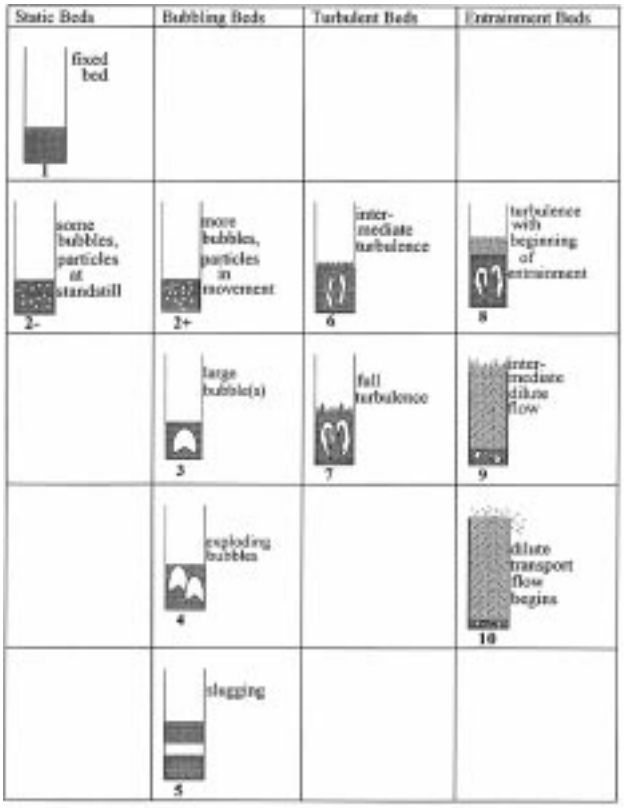

Figure 4. Overview of operation regimes of fluidized beds.

Gas velocity and porosity of bed increase from top to bottom and from left to right.

The point $P_3 = [E_3, M_3, U_3]$ is defined by the maximum of the function of $M^+(E)$ in the interval $\langle E_0, E_{max} \rangle$. Visual observations indicate that this point marks a transition from the bubbling to turbulent regime of fluidization. It can be viewed as the point of incipient (minimum) turbulence of the fluidized bed.

The point $P_4 = [E_4, M_4, U_4]$ denotes a state in which the fluidized bed attains its maximum value of function $E(U)$, or $dE/dU = 0$ and $E_4 = E_{max}$. At this moment, substantial amounts of solids are still in the turbulent regime, and a small but appreciable portion of particles is lifted above the bed. Therefore, this point can be taken as the point where entrainment begins. One should note that all material remains within the column until $U \geq U_{max}$.

The short lines vertical to the characteristic curves of the fluidized bed in Figures 3a and 3b bound the different regimes mentioned and numbered in Figure 4. The function $E(U)$ increases as the gas velocity increases up to the point of beginning entrainment. In this interval, ($[0, U_4]$), the characteristic curve is described by the functions $M^+(E)$ and $E^+(U)$ in Figures 3a and 3b, respectively. When the superficial velocity is further increased, the entrainment becomes more pronounced. The characteristic curve is described by the functions $M^-(E)$ and $E^-(U)$.

As can be seen in Figure 3a, the measure of dominancy, $M^+(E)$, increases with increasing superficial velocity from $U = 0$ to $U = U_3$, where a flat maximum is attained at $E = E_3$ (that is, $dM/dE > 0$, when $dE/dU > 0$). In other words, the maximum dominancy of the amplitude spectrum is reached in the operation point P_3. In contrast to the regimes at lower superficial velocities, both functions $M^-(E)$ and $E^-(U)$ do not change dramatically at higher gas flow rates. The course of the function $M^-(E)$ is considerably influenced by other circumstances at which the entrainment occurs (such as column geometry and material properties of the solids). It is apparent, however, that the function $E^-(U)$ decreases with the increasing superficial velocity.

On analyzing the experimental results, two findings can be noticed: (1) all properties of the described characteristic curve hold for all the conducted experiments, and (2) no other specific property of the characteristic curve occurred in any of the experimental runs.

Therefore, we believe that such characteristic curves can be employed in detecting different operation regimes of fluidized beds. The class of regimes (bubbling beds, turbulent, and entrainment/fast beds) can be determined on the basis of the signs of the derivatives dM/dE and dE/dU according to the following scheme:

1. If $dM/dE > 0$ and $dE/dU > 0$, then bubbling beds occur.
2. If $dM/dE \leq 0$ and $dE/dU > 0$, then turbulent beds exist.
3. If $dE/dU \leq 0$, then entrainment beds occur.

Particular subintervals of $M \in [0.\bar{6}, 1]$ correspond to the respective regimes of fluidization.

It seems to be likely that in the case of binary-mixture beds comprising particles with widely different velocities of minimum fluidization, their characteristic curves will not be as simple as described earlier. For example, if the segregation of particles occurs, the function $E(U)$ might not have a single maximum.

The proposed fluctuation model was also compared with the entirely independent results provided by the separate experiments. An air-velocity–pressure drop relationship for the bed of the same ceramsite particles was measured using simple *U*-manometer. The results are plotted and compared with the results of the fluctuation model in Figure 5. The values of the respective characteristic velocities U_{bf}, U_{mf}, and U_{cf}, determined by this standard method, are in fair agreement with the positions of the points P_1, P_2, and P_3, respectively.

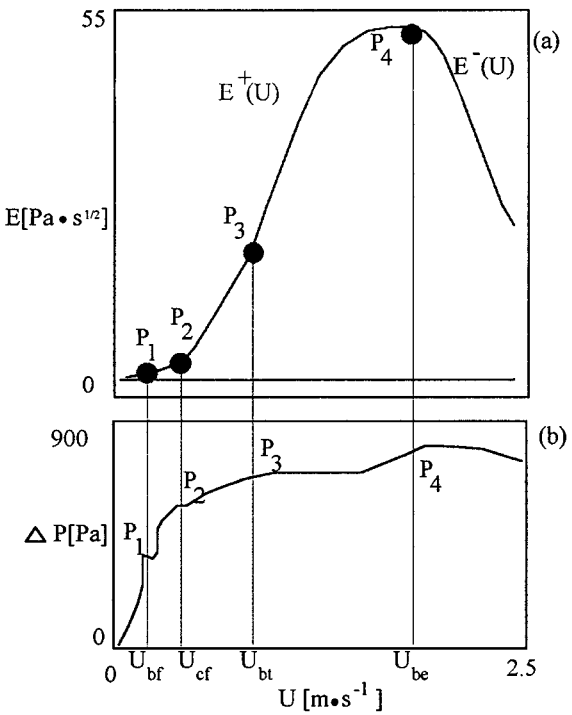

Figure 5. Operation points estimated by the fluctuation model and the independent standard curve ΔP vs. U.

(a) Functions $E^+(U)$ and $E^-(U)$ in the fluctuation model; (b) pressure drop across the bed measured by an independent manometer as a function of gas velocity [results of a separate experimental run with the same material (ceramsite; 0.40–2.40 mm)].

Since the proposed model describes the kinetic states of fluidized systems (regimes), it is not tied to any particular physical properties of materials nor the geometry of the vessel. We believe that the proposed procedure, based on the dependence $M(E)$ and $E(U)$, has a solid basis. Its properties will be explored further in future work, for example, at the systems with continuous throughflow of solids or in which defluidization phenomena occur.

Conclusions

The proposed fluctuation model of the fluidization regimes makes it possible to determine an actual operation regime for the bed at a given moment of time, with the aid of spectral analysis of the fluctuating pressure signal. Compared to measuring the static pressure, this instrumental technique is much more sensitive. It provides pronounced changes in the $E-$quantities in the regions where the static pressure is weakly sensitive to changes in the gas flow rate (onsets of turbulence and entrainment).

Acknowledgment

This work was supported by Grants A4072601 and A4072711 from the Grant Agency of the AS CR and Grant 203/98/0101 from the Grant Agency CR.

Notation

a_i = amplitude pertaining to i-line of spectrum related to time−mean pressure, Pa
d_{pj} = sieve particle size of j-fraction, mm
$E^+(U)$ = quantity $E(U)$ at subentrainment gas velocities, $Pa \cdot s^{1/2}$
$E^-(U)$ = quantity $E(U)$ for gas velocities at which entrainment of particles occurs, $Pa \cdot s^{1/2}$
f_i = frequency pertaining to i-line of amplitude spectrum, Hz
i = index of line in amplitude spectrum
i_M = subscript giving position of median in assorted spectrum
$M^+(E)$ = function describing characteristic curve of fluidized bed at subentrainment gas velocities
$M^-(E)$ = function describing characteristic curve for gas velocities at which entrainment of particles occurs
P = pressure, Pa
ΔP = pressure drop, Pa
U_{be} = gas velocity at beginning of entrainment of particles above the bed (particles remain within the vessel), $m \cdot s^{-1}$
U_{bf} = gas velocity at beginning fluidization of polydisperse system, $m \cdot s^{-1}$
U_{bt} = gas velocity at beginning turbulent fluidization, $m \cdot s^{-1}$
U_{cf} = gas velocity at complete fluidization of polydisperse system, $m \cdot s^{-1}$
U_{mf} = minimum fluidization velocity, $m \cdot s^{-1}$
W = spectral power of fluctuations in chosen band of frequency, $Pa^2 \cdot s$
ρ_p = density of particles, $kg \cdot m^{-3}$

Literature Cited

Bai, D., E. Shibuya, Y. Masuda, N. Nakagawa, and K. Kato, ''Flow Structure in a Fast Fluidized Bed,'' *Chem. Eng. Sci.*, **51**, 957 (1996a).

Bai, D., E. Shibuya, N. Nakagawa, and K. Kato, ''Characterization of Gas Fluidization Regimes Using Pressure Fluctuations,'' *Powder Technol.*, **87**, 105 (1996b).

Brereton, C. M. H., and J. R. Grace, ''The Transition to Turbulent Fluidization,'' *Chem. Res. Des.*, **70**, 246 (1992).

Briens, C. L., L. A. Briens, J. Hay, C. Hudson, and A. Margaritis, ''Hurst's Analysis to Detect Minimum Fluidization and Gas Maldistribution in Fluidized Beds,'' *AIChE J.*, **43**, 1904 (1997).

Catipovic, N. M., G. N. Jovanovic, and T. J. Fitzgerald, ''Regimes of Fluidization for Large Particles,'' *AIChE J.*, **24**, 543 (1978).

Chehbouni, A., J. Chaouki, C. Guy, and D. Klvana, ''Characterization of the Flow Transition Between Bubbling and Turbulent Fluidization,'' *Ind. Eng. Chem. Res.*, **33**, 1889 (1994).

Grace, J. R., ''Contacing Modes and Behaviour Classification of Gas-Solid and Other Two-Phase Suspensions,'' *Can. J. Chem. Eng.*, **64**, 353 (1986).

Grace, J. R., ''High-Velocity Fluidized Bed Reactors,'' *Chem. Eng. Sci.*, **45**, 1953 (1990).

Hartman, M., and V. Veselý, ''Incipient Fluidization at Different Conditions and Free-Fall Velocities of Particles,'' *Encyclopedia of Fluid Mechanics*, Suppl. 2, *Advances in Multiphase Flow*, N. P. Cheremisinoff, ed., Gulf, Houston, p. 137 (1993).

Hartman, M., and R. W. Coughlin, ''On the Incipient Fluidized State of Solid Particles,'' *Collect. Czech. Chem. Commun.*, **58**, 1213 (1993).

Hartman, M., Z. Beran, K. Svoboda, and V. Veselý, ''Operation Regimes of Fluidized Beds,'' *Collect. Czech. Chem. Commun.*, **60**, 1 (1995).

He, Z., W. Zhang, K. He, and B. Chen, ''Modeling Pressure Fluctuations via Correlation Structure in a Gas-Solid Fluidized Bed,'' *AIChE J.*, **43**, 1914 (1997).

Press, W. H., B. P. Flannery, S. A. Teukolsky, and W. T. Vetterling, *Numerical Recipes in Pascal*, Cambridge Univ. Press, Cambridge (1992).

Schouten, J. C., and C. M. van den Bleek, ''Monitoring the Quality of Fluidization Using the Short-Term Predictability of Pressure Fluctuations,'' *AIChE J.*, **44**, 48 (1998).

Svensson, A., F. Johnsson, and B. Leckner, ''Fluidization Regimes in Non-Slugging Fluidized Beds: The Influence of Pressure Drop Across the Air Distributor,'' *Powder Technol.*, **86**, 299 (1996).

Svoboda, K., J. Čermák, M. Hartman, J. Drahoš, and K. Selucký, ''Pressure Fluctuations in Gas-Fluidized Beds at Elevated Temperatures,'' *Ind. Eng. Chem. Process Dev.*, **22**, 514 (1983).

Svoboda, K., J. Čermák, M. Hartman, J. Drahoš, and K. Selucký, ''Influence of Particle Size on the Pressure Fluctuations and Slugging in a Fluidized Bed,'' *AIChE J.*, **30**, 513 (1984).

Xu, G., K. Nomura, Y. Bai, G. Sun, N. Nakagawa, J. Li, and K. Kato, ''Characteristics of Pressure with Respect to Heterogeneous Flow Structure in Fluidized Beds,'' *J. Chem. Eng. Jpn.*, **31**, 236 (1998).

Yates, J. G., and S. J. R. Simons, ''Experimental Methods in Fluidization Research,'' *Int. J. Multiphase Flow*, **20**(Suppl.), 297 (1994).

Manuscript received Jan. 14, 1999, and revision received July 26, 1999.